

30p

N65-89021

~~X64-10984~~

Code 2A

(NASA TMX-50100)

T
STABILITY AND CONTROL FOR THE
MANNED ORBITAL LABORATORY

By Peter R. Kurzhaals

[1963] 30p Ref

Corp. and: NASA Langley Research Center,
Langley Station, Hampton, Va.

Presented at the SAE A-18 Committee Meeting,

Houston, Texas

December 11-13, 1963

Available to NASA Offices and
NASA Centers Only.

STABILITY AND CONTROL FOR THE
MANNED ORBITAL LABORATORY

By Peter R. Kurzhals*

NASA Langley Research Center

SUMMARY

10 984

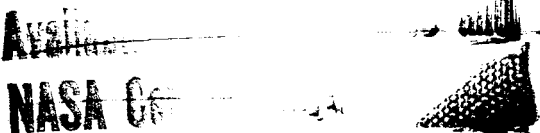
Several manned orbital laboratory concepts originated at the Langley Research Center are outlined, and approximate mass and inertia characteristics for these laboratories are presented. Disturbances and flight-control requirements are discussed and the stability system functions for the laboratories are developed. Typical components for such stability systems are considered and are used to define three stability systems suitable for both zero-gravity and artificial-gravity laboratories. Comparative results for these systems are then presented for a cylindrical manned orbital laboratory having both spinning and nonspinning modes of operation, and the effectiveness of the systems under consideration is evaluated. Current experimental research programs which will be used to substantiate the theoretical results and to investigate mechanization problems for these systems are also described.

AUTHOR

INITIAL MANNED SPACE STATIONS

The manned orbital laboratory presents unique problems in the stability and control area. To visualize these problems let us briefly look at some early configurations which are shown in figures 1 and 2. Figure 1 illustrates an erectable 30-foot rotating space station which consists of a rigid central module and an inflatable outer section. Gemini vehicles would be used for

*Head, Stability and Control Section, Space Station Research Group.



rendezvous, and station power would be derived from a parabolic solar collector. Because of the solar collector, the 30-foot station must be stabilized to point within half a degree of the sun. The station stability system must thus compensate for internal crew motions, gravity gradient torques, docking torques, and similar disturbances to hold this accuracy.

The 150-foot station in figure 2 has six cylindrical outer modules arranged in the shape of a hexagon. These outer modules are connected to the central hub and docking port by three spokes. Solar panels now produce the necessary station power. To function efficiently, these solar panels must point within about 10° of the sun, so that the station stability system must again compensate for internal and external disturbances to hold this attitude.

Assumed characteristics for these two rotating space stations are shown in figure 3. The normal orbital weights are 8,100 pounds for the 30-foot station and 137,000 pounds for the 150-foot station, and the stations would house crews of 2 and 21 astronauts, respectively. Spin and inplane inertias for the two stations are also given, and artificial gravity levels of 0.5g and 0.2g would be provided by respective spin rates of 10 and 3 rpm.¹

External disturbances for these laboratories can in general be compensated for by means of small jets spaced on the periphery of the station.² Internal disturbances, which are represented in figure 4, are a different problem, however. This figure presents the effects of various crew motions and docking impacts in terms of the station maximum wobble angle and the apparent station rolling. Here the 30-foot station with wobble angles of up to 108° presents a serious problem and will require extensive stabilization. The 150-foot station in comparison has maximum wobble angles of about 3° and thus is essentially spin stabilized.³

Since the dynamic unbalances resulting from crew motions produce by far the largest attitude errors and since these disturbances will occur continuously, the rotating stations will use momentum wheels or passive damping devices to compensate for these internal torques. Theoretical and experimental investigations of such a momentum wheel device, the double-gimbaled control moment gyro, have been completed and will be applied to a manned orbital laboratory in a later section of this paper.^{4,5,6,7} Passive damper studies aimed at the determination of an optimum passive damper concept are also underway.⁸ From the results available at present, it appears that stabilization of these rotating stations is within the state of the art.

MANNED ORBITAL LABORATORY

The function of the stability system thus far has been relatively simple and only requires an attitude hold capacity within certain limits. For the laboratory shown in figure 5, this control function becomes somewhat more involved. The manned orbital laboratory or MOL consists of a cylindrical module attached to the last stage of its launch vehicle. The laboratory is intended for both zero-gravity and artificial-gravity operations, and the zero-gravity mode is illustrated in the figure. For artificial gravity or spinning operation, the laboratory is spun up slowly and the booster is then let out using an eight-cable arrangement. At the same time, jets on the laboratory and booster accelerate the laboratory to its final spin rate.⁹

Assumed specifications for this laboratory are shown in figure 6. The orbital weight of the laboratory and booster combination is about 76,000 pounds and the laboratory will have a normal crew of six. The inertias are cylindrical with an X or minimum axis of inertia of 190,000 slug-ft² for both the

nonspinning and spinning modes. The Y-axis inertias are 2,000,000 and 21,000,000 slug-ft² and the Z-axis inertias are 2,010,000 and 21,010,000 slug-ft² for the two modes. A normal spin rate of 3.73 rpm is anticipated about the Z-axis, which is the axis normal to the solar panels.

Flight-Control Requirements and Components

Before we consider the stability and control problem for this laboratory, we shall review the characteristic flight-control requirements shown in figure 7. This figure lists the maneuver requirements and maximum allowable errors for the initial activation of the unmanned laboratory, for rendezvous, for zero-gravity and experimental operation, and for artificial-gravity operation. Rates of 0.5 deg/sec and accelerations of 0.5 deg/sec² should be obtainable during the nonspinning modes, while spin rates of 6 to 24 deg/sec with spinup accelerations of 1 deg/sec² are needed. The allowable errors in the nonspinning mode vary from 10 deg and 0.1 deg/sec in the activation phase to 0.1 deg and 0.02 deg/sec for photographic missions. During the spinup mode maximum damped wobble angles of 6 deg and damped wobble rates of 5 deg/sec are acceptable.

With these requirements in mind a number of stability systems were investigated, and typical components for these systems are presented in the next figures. For the nonspinning mode of operation we have primarily reaction wheels and control moment gyros. A reaction wheel, illustrated in figure 8, is simply a flywheel which is accelerated by means of a torquer to exert a laboratory control torque about the spin axis of the flywheel. In comparison, the control moment gyro, shown in figure 9, produces a torque by the precession of a constant-rate wheel which is mounted on gimbals. For example, if we apply a torque to the outer gimbal of the wheel on the right of the figure, an equal and opposite torque will act on the laboratory and the wheel will precess about

the inner gimbal. The control torque can be applied until the wheel gimbal angle reaches a saturation limit, which is usually about 60° or 70° . A number of modifications of this basic idea are possible since we can use single or double gimbals for either one wheel or for two wheels spinning in opposite directions. The figure shows one of the more sophisticated versions, a double-gimbaled twin control-moment gyro. Either a gimbal torque or a gimbal rate can be commanded to yield the desired laboratory control.

For the spinning mode, as described in figure 10, we are concerned with a constant-rate single control wheel on double gimbals. Control torques are derived from the precession moments resulting from a misalignment of the wheel spin vector with the laboratory spin axis. It can readily be seen that a double-gimbaled CMG offers immediate advantages for the manned laboratory, since the same system can be used for both nonspinning and spinning modes by merely changing the control logic input to the gimbal torquers.

Typical Control Systems

Using these components as building blocks, we can next define an optimum stabilization system for the manned orbital laboratory. Such an optimum system should satisfy the previously specified flight-control requirements at a minimum size, weight, and power cost. Three basic control concepts have been investigated at the Langley Research Center, and control logic and torque equations for each of these systems have been derived. The resulting expressions were combined with the laboratory equations of motion and were solved on an IBM 7090 computer to evaluate the control system performance.

The three systems being studied are described in figures 11 to 13. The first system, shown in figure 11, has two twin control-moment gyros with a total angular momentum of 3,370 ft-lb-sec. These provide torques about all

axes of the laboratory in the nonspinning mode. One set of the gyro wheels is alined with the X or minimum inertia axis and the other set of wheels is alined with the Z-axis or the axis normal to the solar panels. Control torques are produced on the MOL by commanding torques on the double gimbals supporting each wheel.

For spinning operation, the two wheels alined with the X-axis are precessed through 90° until their spin vector coincides with the laboratory positive Z or spin axis. Simultaneously, the wheel alined with the negative Z-axis is despun. This results in three single control-moment gyros having their spin vector parallel to the laboratory spin vector. Gimbal rates and angles are now commanded for each of these wheels to provide the necessary damping torques. In addition, on-off jets are used for CMG desaturation and control in the non-spinning modes and for spinup and attitude control in the spinning mode.

The second control concept is shown in figure 12. During zero-gravity operation, this system uses a single double-gimbaled control-moment gyro for X- and Y-axis control and a single-gimbaled twin control-moment gyro for Z-axis control. These gyros are now rate controlled, which means that a gimbal rate command is fed to the gimbal torquers. For artificial-gravity operation, precession of the twin CMG yields one double-gimbaled and two single-gimbaled wheels alined with the Z-axis. Pulse jets are used for supplementary control operations, as before.

The third control concept, presented in figure 13, has a twin double-gimbaled CMG giving Y- and Z-axis control torques and a reaction wheel giving X-axis control torques in the nonspinning mode. Control commands call for torques on the reaction wheel motor and the gimbal torquers. In the spinning

mode the twin CMG wheels are aligned with the Z-axis; and on-off jets are again employed for both modes.

Comparative Results

To evaluate the relative effectiveness of these systems, a standard of comparison must be selected. Here this standard was taken as the total angular momentum capacity of each system, that is, all systems studied had an equal amount of angular momentum available before saturation. Let us then look at some typical results on the laboratory control with these systems. The non-spinning mode performance is given in figure 14 for a maneuver command of 5° in roll, pitch, and yaw. The time histories give the resultant laboratory attitude errors in degrees plotted versus time in minutes. Systems I and III can be seen to readily achieve the desired attitude to within the 0.1° accuracy specified by the flight-control requirements. System II, however, provides less effective control and does not attain the final desired accuracies within the time period considered.

More important than these time histories, though, is the percent of saturation of the control system, as this percentage is most indicative of the overall system performance. Here it is apparent that system I, the dual twin CMG system, with 4.58 percent has a greater control capacity than system II or III with 9.54 percent and 5.03 percent, respectively.

The control system performance in the spinning mode is represented by figure 15, which shows the MOL response to products of inertia resulting from the instantaneous movement of three crew members to one end of the laboratory module. As can be seen from the roll and pitch rates, effective damping is obtained from all three systems and the damped conditions, corresponding to

constant rates, are within the control specifications. System I produces somewhat smaller residual attitude errors and damping times than system II or III. This is a direct result of the slightly higher angular momentum available for wobble damping in the dual twin CMG system. Some of the components for the other two systems, such as the reaction wheel and the single-gimbaled CMG set are not as efficient during spinning MOL operation.

CURRENT RESEARCH PROGRAMS

The theoretical data that have been presented here are characteristic of the general trend of the computer data. To substantiate these data and to investigate the practicality of the suggested stability and control systems, two additional research programs have been initiated.

Flight Simulator

The first of these involves the development of a flight simulator which reproduces the MOL control console and manual actuators, as shown in figure 16. This control console is linked to an analog computer which continually solves the laboratory equations of motion with the stabilization torques applied by the pilot. Attitude, rate, and required torque data will be displayed on the console and will be used by the pilot in his control procedure. This flight simulator, which will be operational in January 1964, will determine man's capability to manually control the laboratory during both normal mission maneuvers and during emergency conditions. It will also provide information on optimum console displays for the manual control mode.

Control Flight Test System

The second research program involves three-degree-of-freedom flight table tests of full-scale integrated stability systems for the MOL. A schematic for this test concept is given in figure 17. During a typical test the mission flight profile or disturbance torque is fed into a real-time dynamics computer through a control console. The computer solves the laboratory equations of motion with this input and determines the laboratory angular position and rate. These position and rate commands are transmitted to the gimbal torque motors, which then derive the test table to the corresponding position. The table thus undergoes the same motions as the actual laboratory. The sensor package of the prototype MOL control system now detects the motion of the table with respect to an external sensor reference, and the sensor signals are monitored by an onboard computer which generates wheel and jet command signals. The wheel command signals are fed to the torquers driving control system actuators such as CMG's and reaction wheels. The movement of the actuators exerts laboratory control and damping torques, which are measured by means of force gages and are transmitted back to the dynamics computer. The jet command signals, which may call for maneuver or wheel desaturation torques, are simultaneously fed to a fixed jet facility containing either the actual or a simulated propulsion system. The resultant torques are then sent to the dynamics computer. The computer reappraises the laboratory equations of motion with the new disturbance and stability torque input, and calls for the changes in the table position. This completes the cycle. Manual input can also be provided by pilot-operated control sticks, which will transmit control signals directly to the wheel actuators and jets. The MOL flight simulator discussed previously could be used for this purpose.

A sketch of the flight test table for this test system is shown in figure 18. This table consists of a mounting platform, which is supported by a three-axis orthogonal gimbal arrangement. Continuous rotation of the outer gimbal allows simulation of both spinning and nonspinning laboratory operations. Sensors, instrumentation, and prototype actuators are mounted on the test platform and are linked to the dynamics computer by means of a slipring system.

The data derived from experiments with this flight test system will allow the determination of the control system sensor and actuator effectiveness. In addition, the mechanical operation of the integrated stability and control system can be investigated for a wide range of flight conditions.

CONCLUDING REMARKS

The control test system and the flight simulator discussed here will be used in extensive investigations of MOL stabilization systems. Results from these experiments and the data obtained from previous tests and computer solutions of the laboratory equations of motion will then be combined to give an optimum and reliable control concept for the manned orbital laboratory. At present no major difficulties are foreseen in this task, and the solution of anticipated stability and control problems appears to be within the state of the art.

REFERENCES

1. Kurzahls, Peter R., and Adams, James J.: Dynamics and Stabilization of the Rotating Space Station. Astronautics, vol. 7, no. 9, September 1962, pp. 25-29.
2. Exotech Incorporated Progress Reports: Investigation of Attitude Control for Sun-Oriented Space Stations. Contracts NASw-720 and NASw-780, 1962-1963.
3. Kurzahls, Peter R., Adams, James J., and Hodge, Ward F.: Space Station Dynamics and Control. NASA TN D-1504, 1962, pp. 71-85.
4. Kurzahls, Peter R., and Keckler, Claude R.: Spin Dynamics of Manned Space Stations. NASA TR R-155, 1963.
5. Adams, James J.: Study of an Active Control System for a Spinning Body. NASA TN D-1905, 1961.
6. Adams, James J.: Experimental Study of an Active Control System for a Spinning Body. NASA TN D-1515, 1962.
7. Shearin, John G., and Kurzahls, Peter R.: Stability and Control of Manned Rotating Space Stations. Paper presented at the Ninth Annual American Astronautical Society Meeting of the Interplanetary Missions Conference, January 1963.
8. Space Technology Laboratory Progress Reports: Preliminary Study and Design of Passive Dampers for a Manned Rotating Space Station. Contract NAS 1-3400, 1963.
9. Sperry Gyroscope Company Progress Reports: Stability and Control for a Flexibly-Coupled Rotating Space Station. Contract NAS 1-2946, 1963.

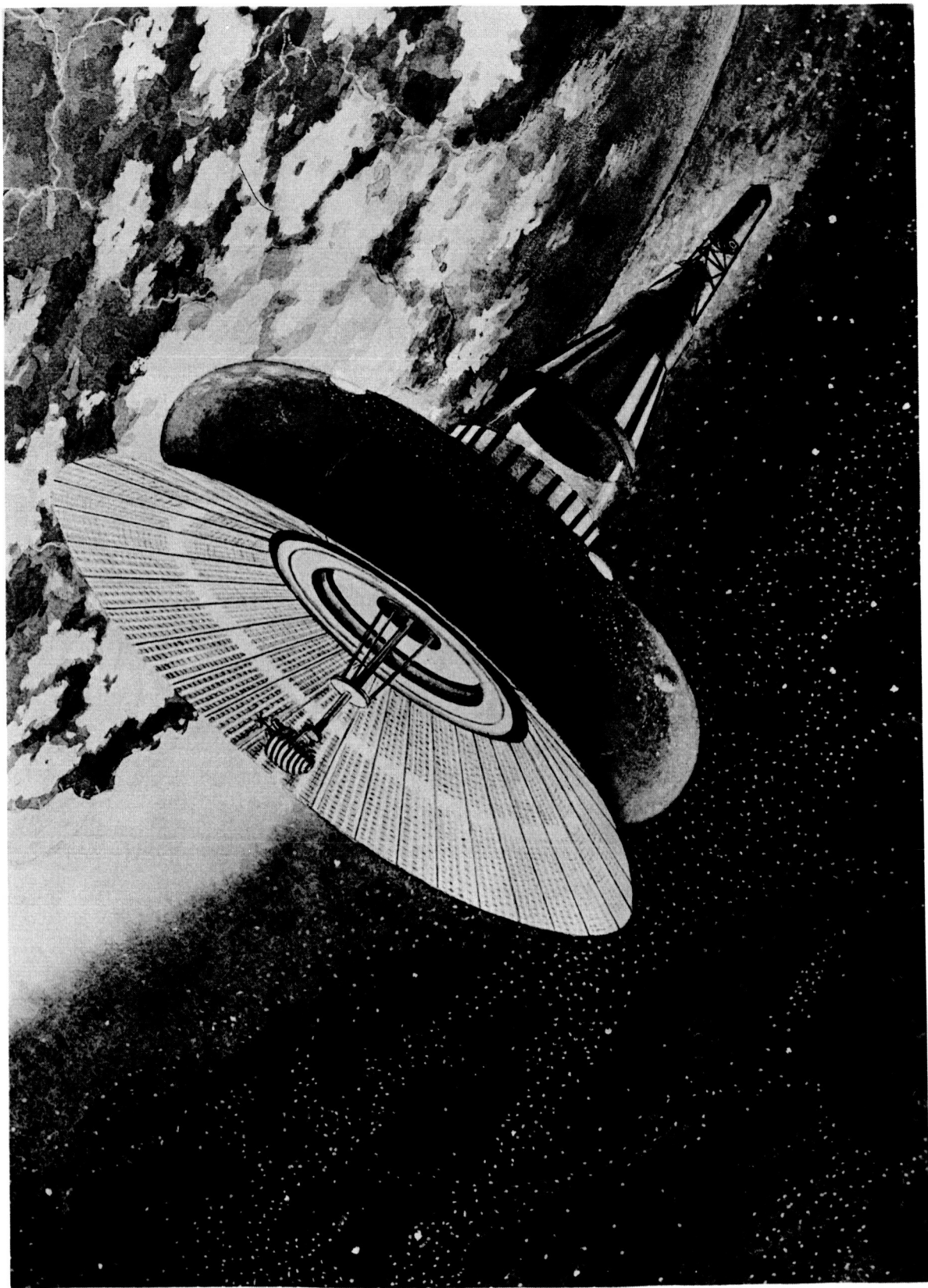


Figure 1.- Artist's concept of a 30-foot erectable space station.

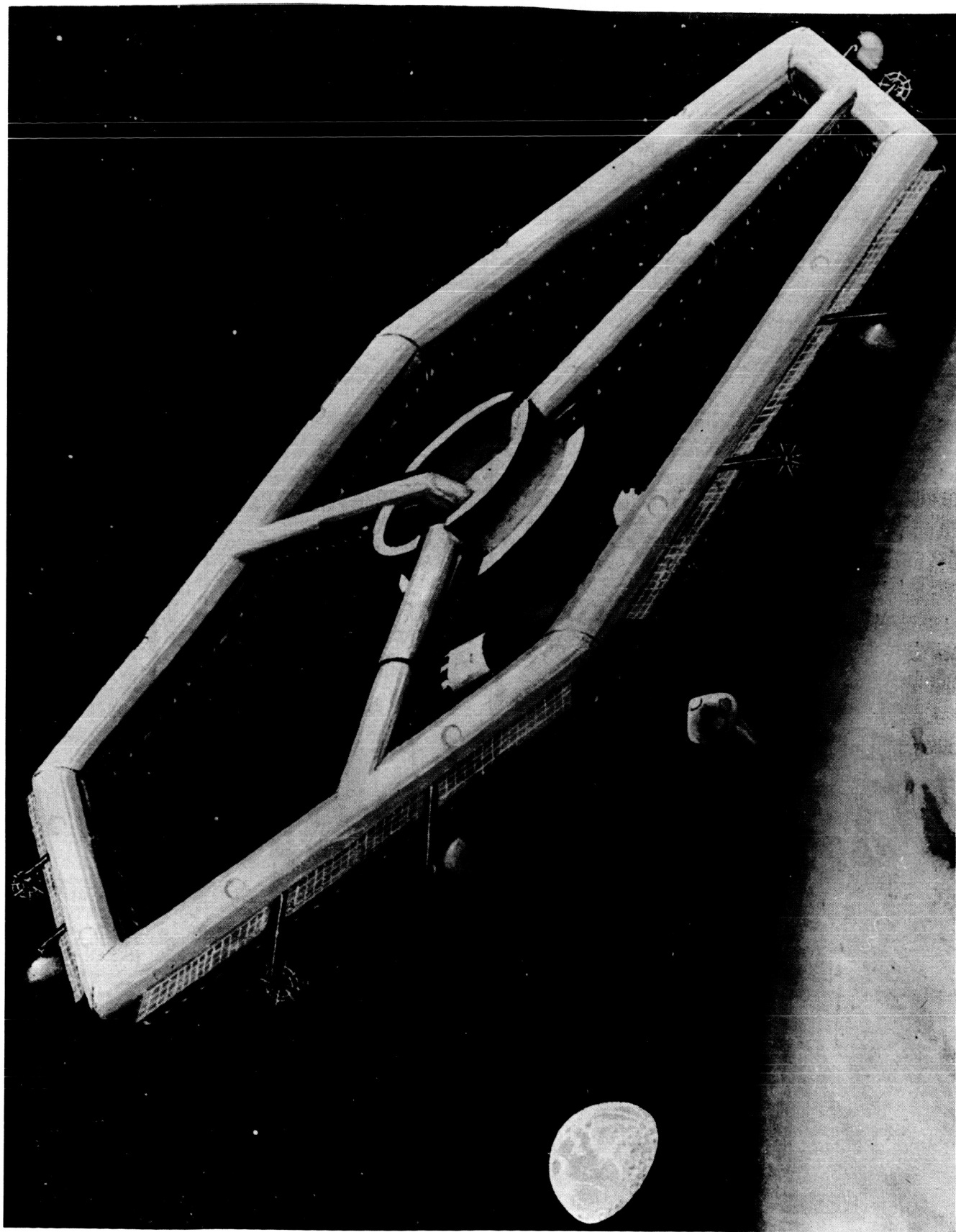


Figure 2.- Artist's concept of a 150-foot hexagonal space station.

	30-FOOT STATION	150-FOOT STATION
ORBITAL WEIGHT, LB	8,100	137,000
INPLANE INERTIA, SLUG FT ²	7,500	10,500,000
SPIN INERTIA, SLUG FT ²	10,000	15,000,000
SPIN RATE, RPM	10	3
CREW	2	21

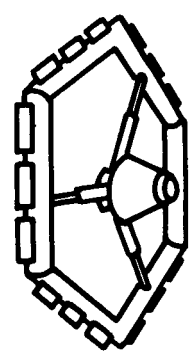
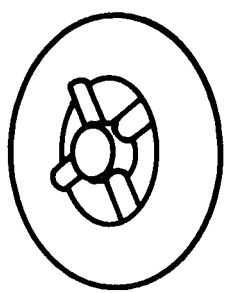


Figure 3.- Assumed specifications for manned rotating space stations.

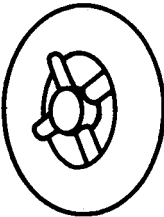
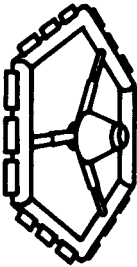
30-FOOT STATION		150-FOOT STATION		
				
CREW : 2		CREW : 21		
TYPE OF DISTURBANCE	DISTURBANCE EFFECTS			
	MAX WOBBLE ANGLE, DEG	APPARENT STA. ROLLING, DEG	MAX WOBBLE ANGLE, DEG	APPARENT STA. ROLLING, DEG
RADIAL CREW MOTIONS	9	0 TO 12	0.7	0 TO 0.8
TRANVERSE CREW MOTIONS	13	0 TO 5	1	0 TO 0.3
CIRCUMFERENTIAL CREW MOTIONS	108	80 TO -80	3	3 TO -3
DOCKING IMPACTS	2	2 TO -2	0.05	0 TO 0.04

Figure 4.- Internal disturbance effects on manned rotating space stations.

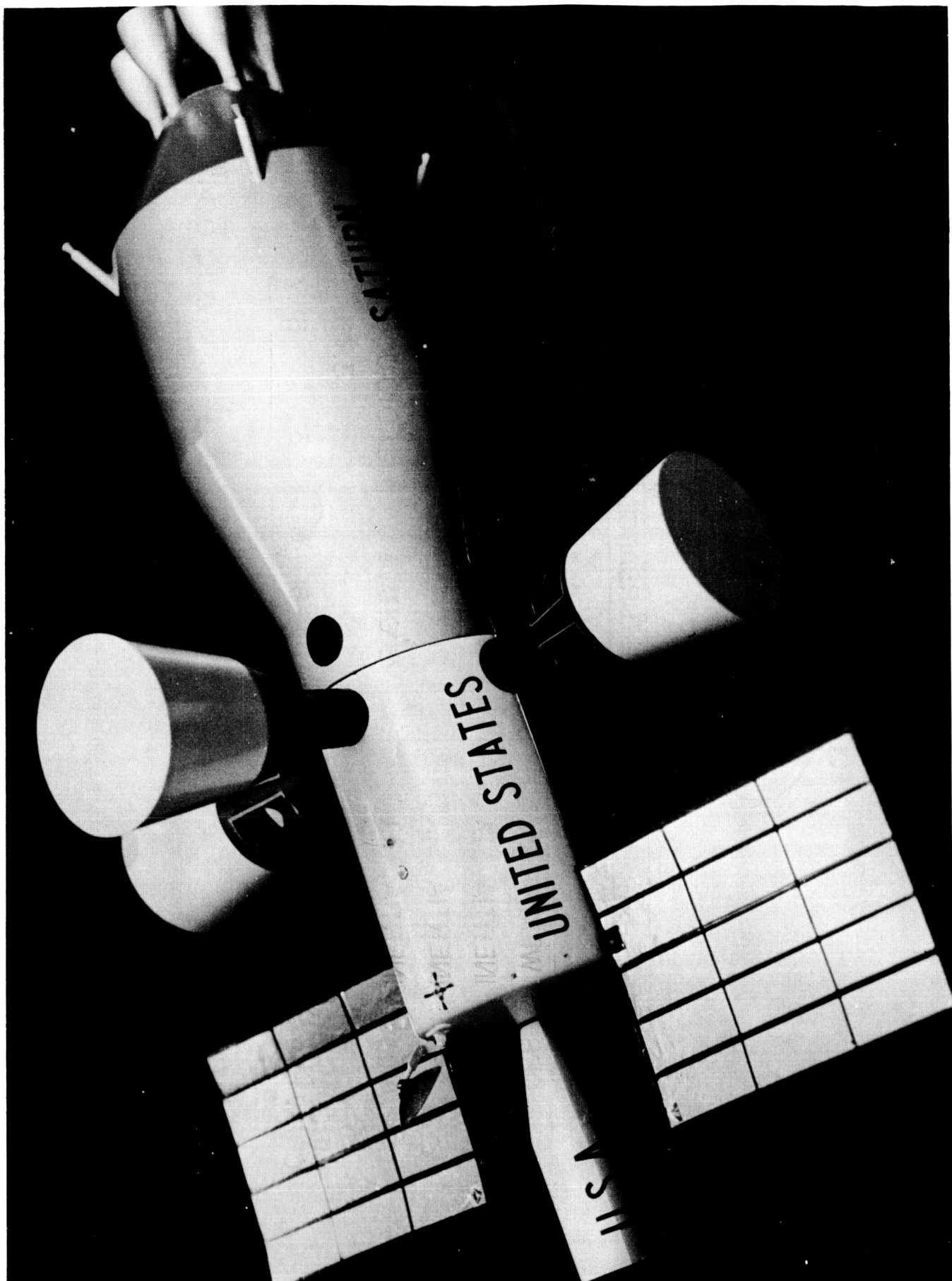

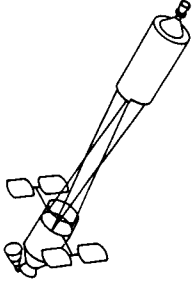


Figure 5.- Model of a cylindrical manned orbital laboratory.

	NONSPINNING	SPINNING
		
ORBITAL WEIGHT, LB	76,000	76,000
X-AXIS INERTIA, SLUG-FT ²	190,000	190,000
Y-AXIS INERTIA, SLUG-FT ²	2,000,000	21,000,000
Z-AXIS INERTIA, SLUG-FT ²	2,010,000	21,010,000
SPIN RATE, RPM	—	3.73
CREW	6	6

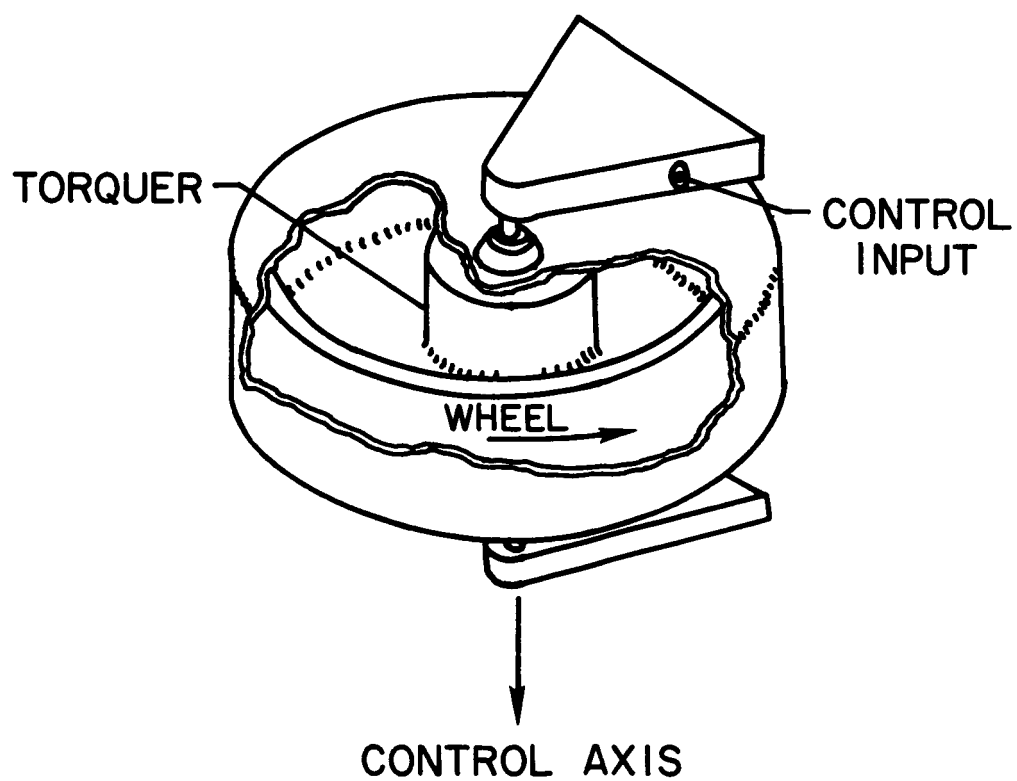
NASA

Figure 6.- Assumed specifications for the manned orbital laboratory.

PHASE	MANEUVER REQUIREMENTS			ALLOWABLE DEVIATION	
	RATE, DEG/SEC	ACCELERATION, DEG/SEC ²	ATTITUDE, DEG	RATE, DEG/SEC	
ACTIVATION	0.5	0.5	10.0	.1	
RENDEZVOUS	0.5	0.5	0.5	0.1	
ZERO G	0.5	0.5	1	0.1	
EXPERIMENTS	0.5	0.5	0.1	0.02	
ARTIFICIAL G	6 TO 24 SPIN	1 SPIN	6 WOBBLE	5 WOBBLE	

NASA

Figure 7.- Flight control requirements for the manned orbital laboratory.



NASA

Figure 8.- Sketch of reaction wheel for nonspinning MOL.

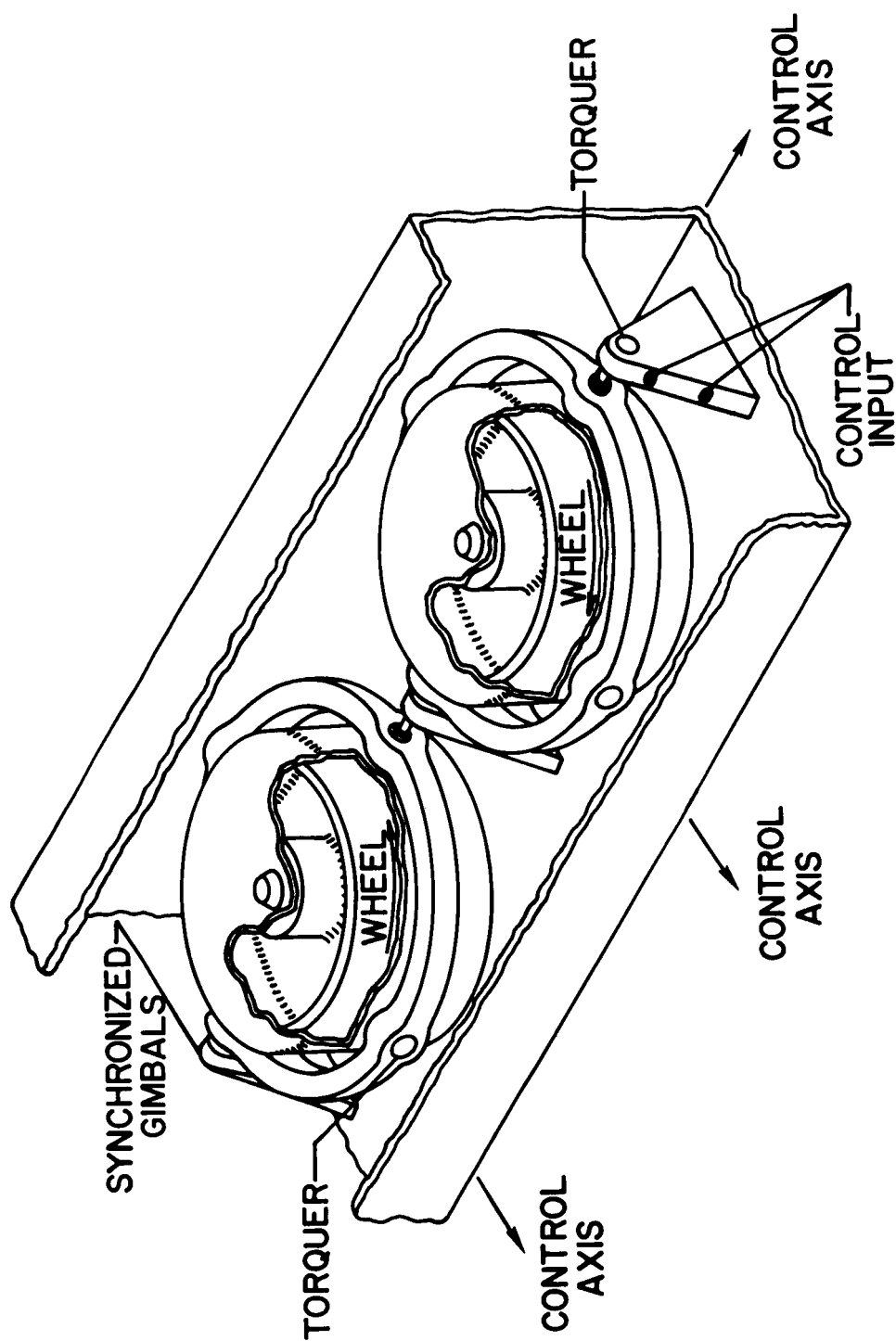
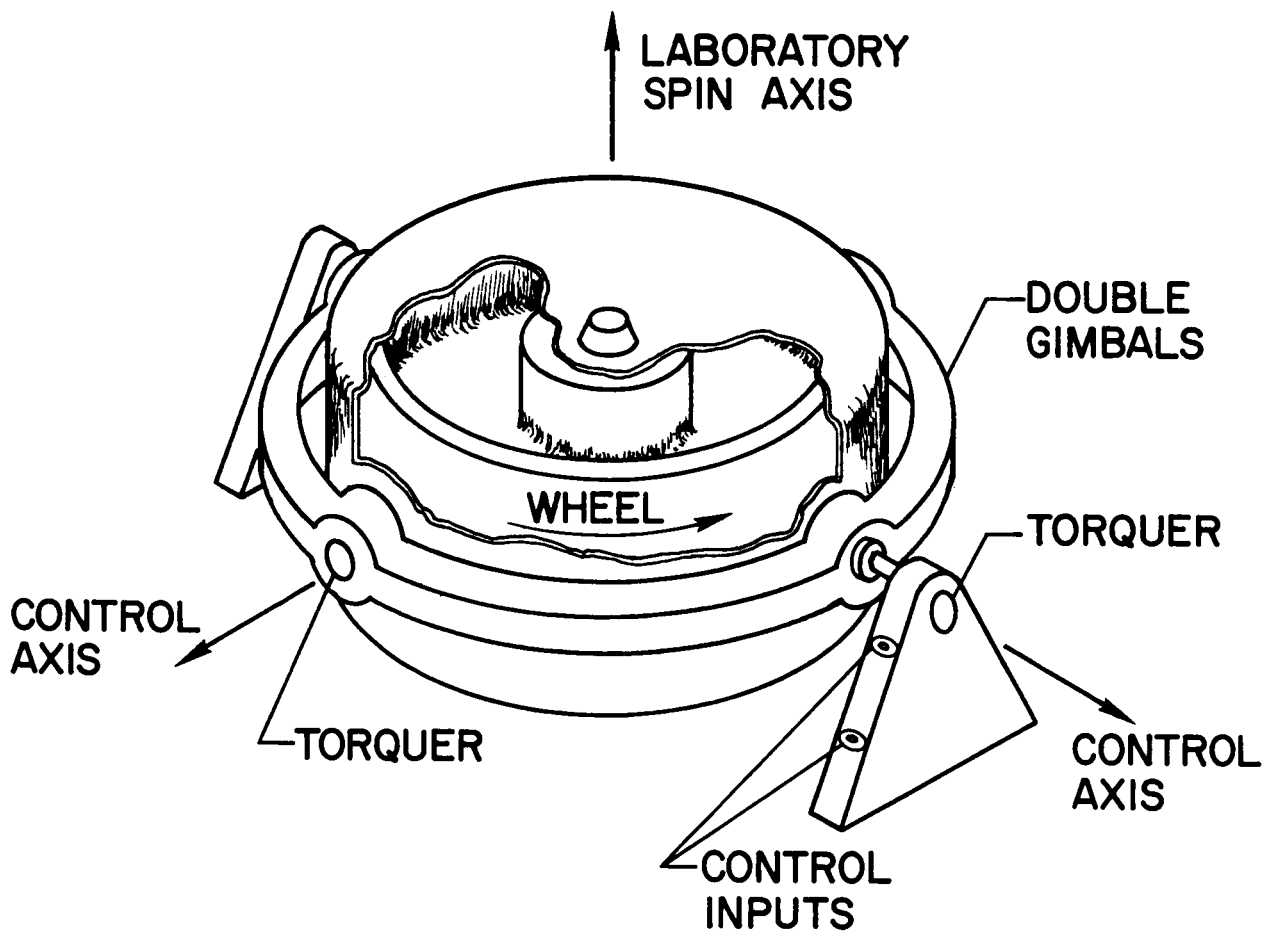


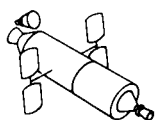
Figure 9.- Sketch of twin CMG for nonspinning MVL.



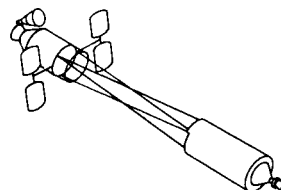
NASA

Figure 10.- Sketch of single CMG for spinning MOL.

NONSPINNING



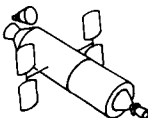
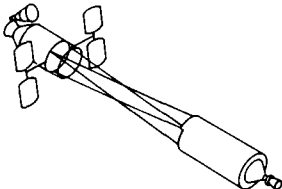
SPINNING



PROPERTY	COMPONENTS				
	TWIN CMG	PULSE JET	SINGLE CMG	PULSE JET	SPIN JET
NUMBER	2	12	3	8	4
CONTROL AXIS	ALL	ALL	X & Y	X & Y	Z
CONTROL COMMAND	TORQUE	TORQUE	RATE ANGLE	TORQUE	RATE
MOMENTUM FT-LB-SEC	3370	—	3224	—	—
THRUST, LB	—	60 200	—	60	200

NASA

Figure 11.- Control system I for MOL.

NONSPINNING				SPINNING		
						
PROPERTY	COMPONENTS					
	SINGLE CMG	TWIN CMG	PULSE JET	SINGLE CMG	PULSE JET	SPIN JET
NUMBER	1	1	8	3	6	6
CONTROL AXIS	X & Y	Z	ALL	X & Y	X & Y	Z
CONTROL COMMAND	RATE	RATE	TORQUE	RATE, ANGLE	TORQUE	RATE
MOMENTUM, FT-LB-SEC	1224	2146	—	2296	—	—
THRUST, LB	—	—	5 50	—	5 50	50

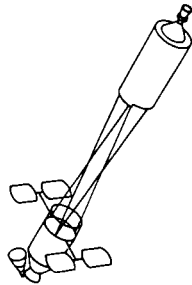
NASA

Figure 12.- Control system II for MOL.

NONSPINNING



SPINNING



PROPERTY	COMPONENTS				
	TWIN CMG	REACTION WHEEL	PULSE JET	SINGLE CMG	SPIN JET
NUMBER	1	1	12	2	4
CONTROL AXIS	Y & Z	X	ALL	X & Y	Z
CONTROL COMMAND	TORQUE	TORQUE	TORQUE	RATE, ANGLE	RATE
MOMENTUM, FT-LB-SEC	3100	270	—	3100	—
THRUST, LB	—	—	60 200	—	200

NASA

Figure 13.-- Control system III for MOL.

DISTURBANCE, SLUG - FT ²	SYSTEM LEGEND	TIME TO DAMP, MIN.	DAMPED ATTITUDE, DEG.
$I_{xy} = 9,735$	I - DUAL TWIN CMG	I - 1.10	I - $3.27 \pm .025$
$I_{xz} = -9,735$	II - TWIN CMG & SINGLE CMG	II - 1.20	II - $3.82 \pm .025$
$I_{yz} = -1,040$	III - TWIN CMG & REACTION WHEEL	III - 1.12	III - $3.34 \pm .025$

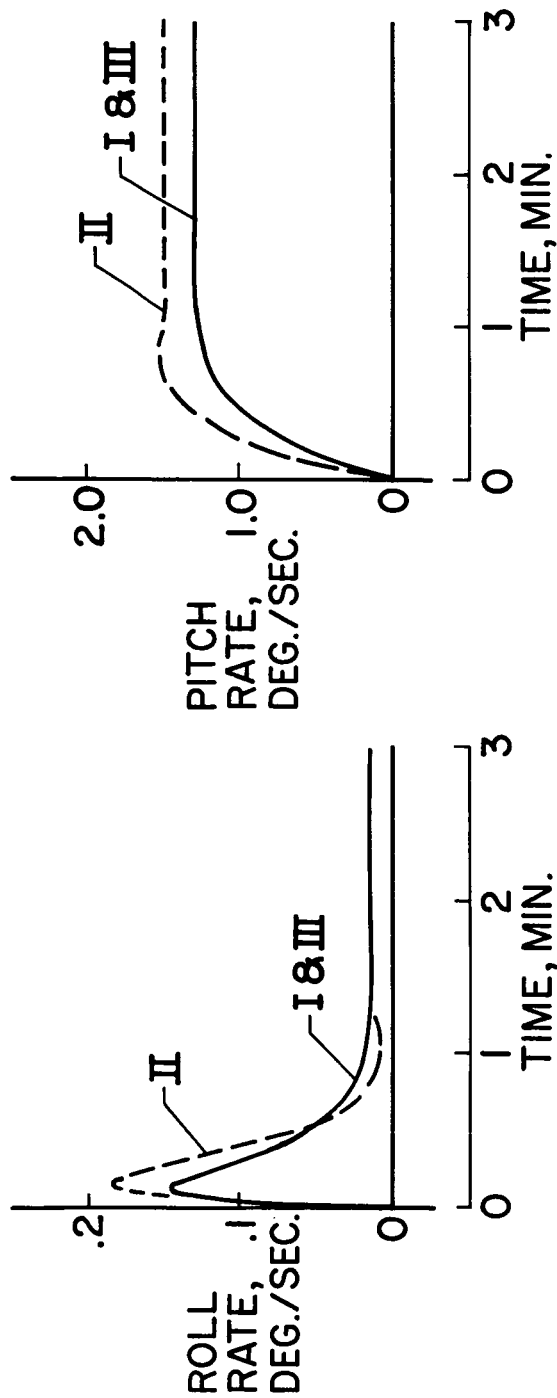


Figure 14.- Comparative control system performance for nonspinning MOL.

MANEUVER COMMAND	
5° ROLL	
5° PITCH	
5° YAW	
SYSTEM LEGEND	
I-DUAL TWIN CMG	
II-TWIN CMG AND SINGLE CMG	
III-TWIN CMG AND REACTION WHEEL	
PERCENT OF SYSTEM SATURATION	
I 4.58 %	
II 9.54 %	
III 5.03 %	

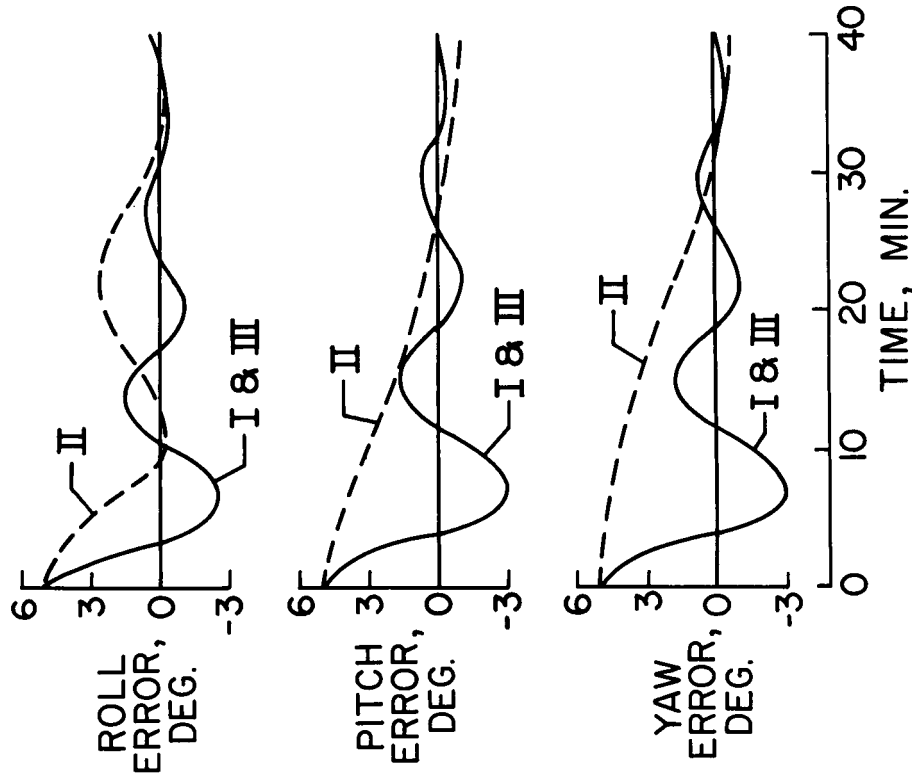
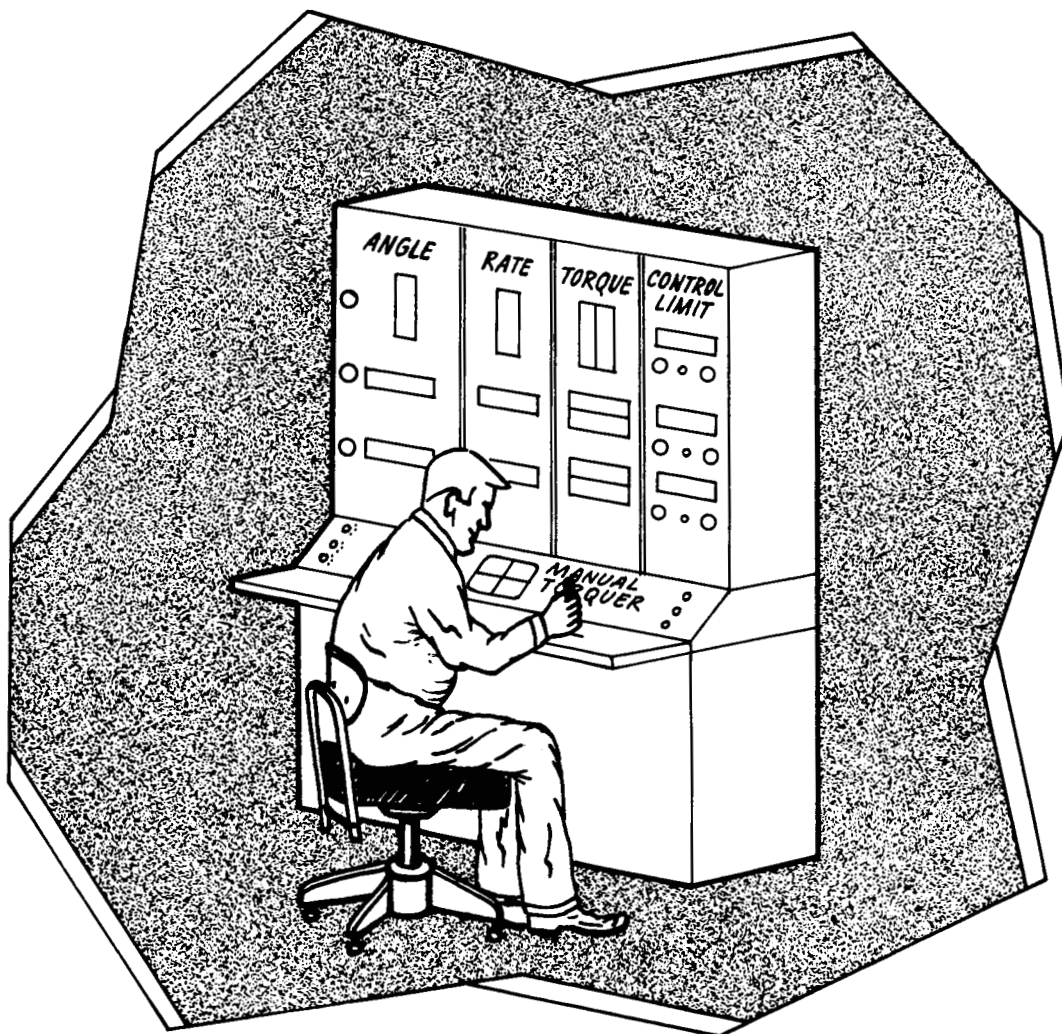


Figure 15.- Comparative control system performance for spinning MOL.



NASA

Figure 16.- Sketch of MOL control console.

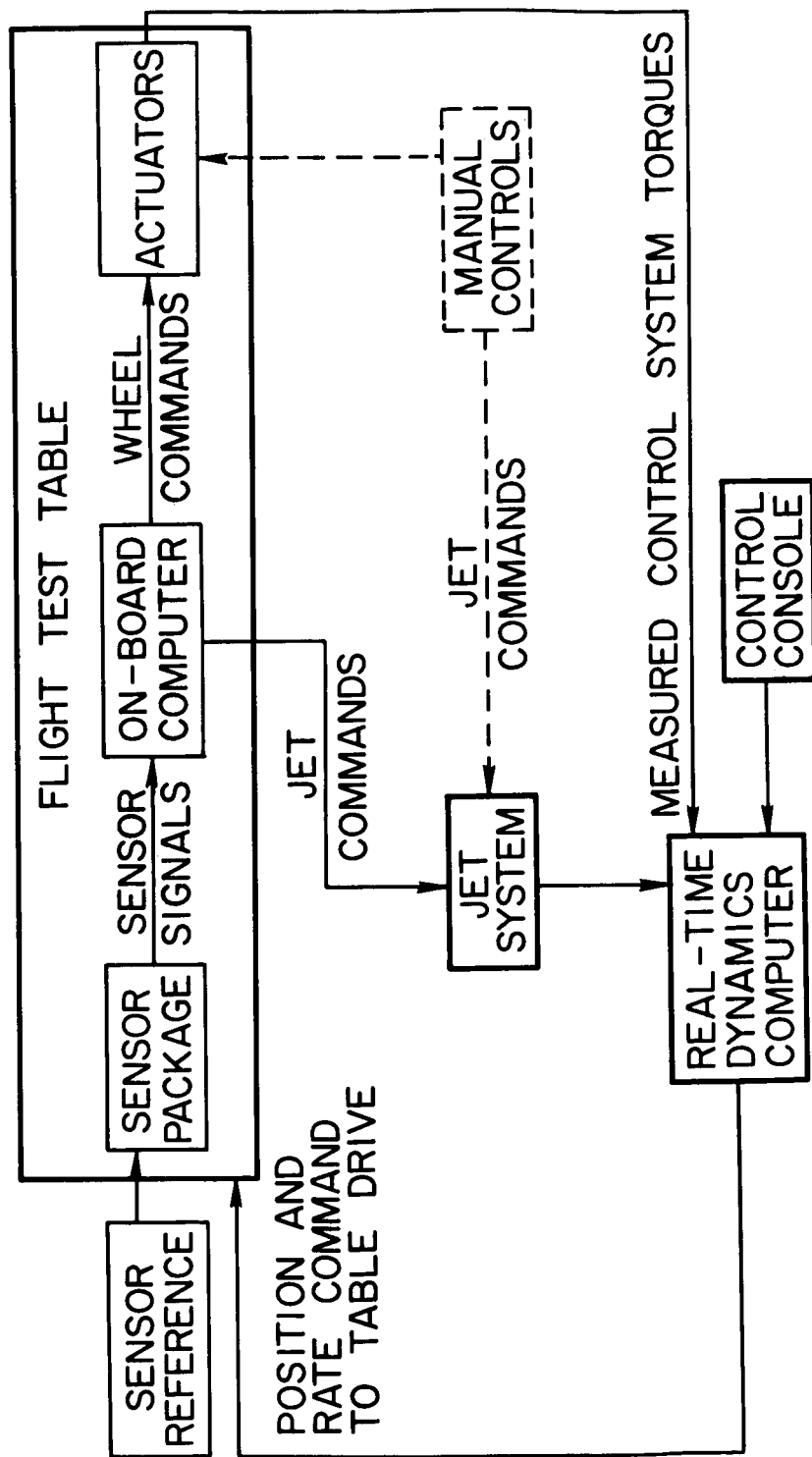


Figure 17.- Schematic of control flight test system.

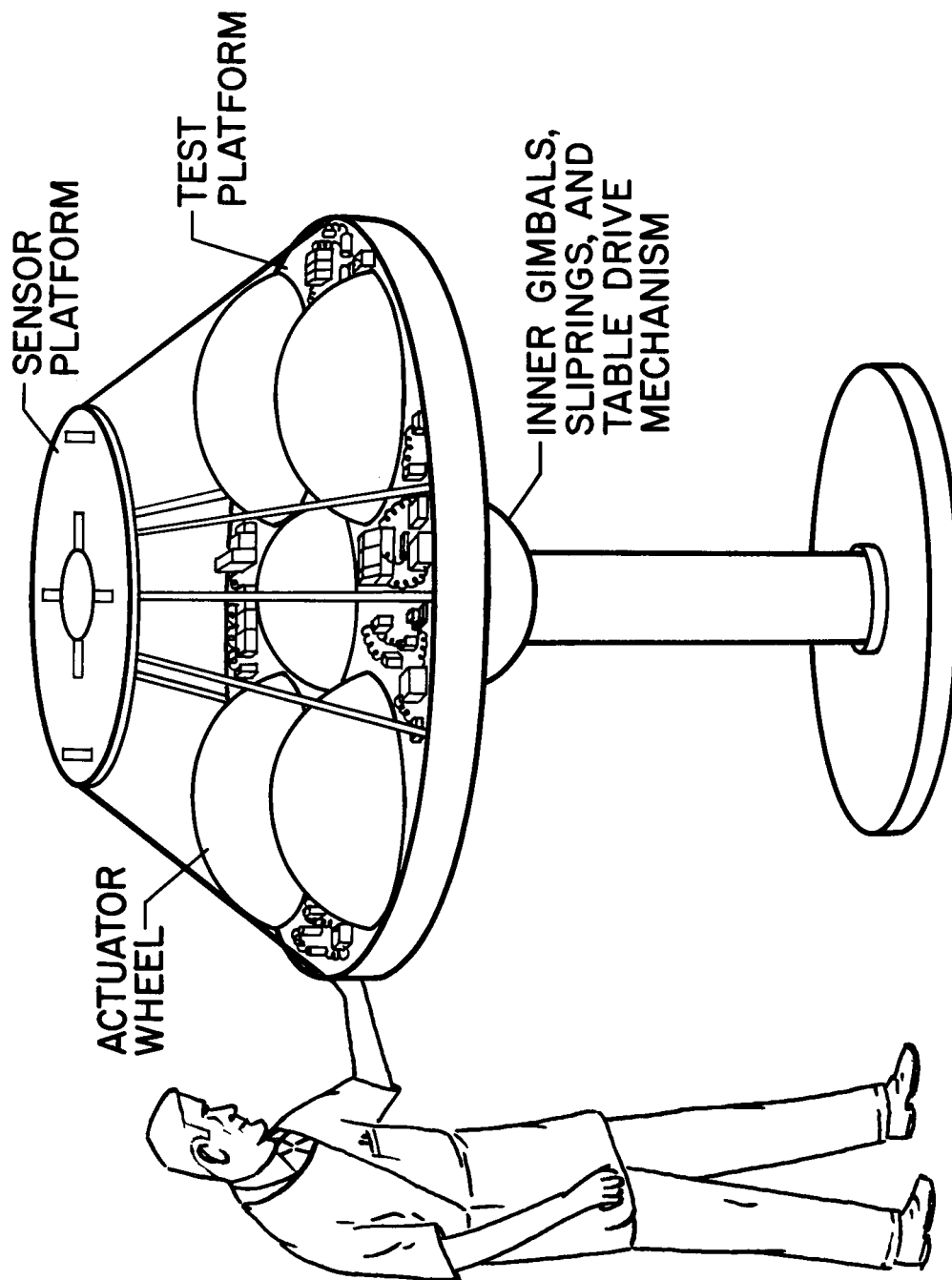


Figure 18.- Sketch of MOL control test table.